Electronic Supplementary Material (ESI) for Soft Matter.

Electronic Supporting Information: Flow and Arrest in Stressed Granular Materials

Ishan Srivastava

Center for Computational Sciences and Engineering,

Lawrence Berkeley National Laboratory, Berkeley, CA 94720, USA

Leonardo E. Silbert

School of Math, Science, and Engineering,

Central New Mexico Community College, Albuquerque, NM 87106, USA

Jeremy B. Lechman and Gary S. Grest

Sandia National Laboratories, Albuquerque, NM 87185, USA

STEADY STATES OF FLOW AND ARREST AT DIFFERENT PRESSURES

The steady states of flow and arrest described in the main text correspond to an external applied pressure of $p_a = 10^{-5}$. In this Supporting Information we calculate similar states for a higher and a lower applied pressure: $p_a = 10^{-4}$ and $p_a = 10^{-6}$. Additionally, we also extract the critical values at the flow-arrest transition boundary at these applied pressures, which are shown in Fig. S3. In Figs. S1 and S2, we show all simulated steady states of shear arrest (open symbols) and shear flow (closed symbols) for all simulated interparticle frictions μ_s along various axes described in Figs. 2 and 3 of the main text. Evidently the states of flow and arrest and the boundary defining the flow-arrest transition are similar for all pressures, thus confirming our assumption that the present results correspond to a hard-particle limit. At lower pressures (corresponding to stiffer particles), the stress-controlled simulation method requires substantially longer simulation runs to achieve steady state and to extract reasonable statistics concerning the material microstructure. This is seen by the large error bars associated with identifying a_c^c and Z_c for the the case of $p_a = 10^{-6}$ in Fig. S3. Furthermore, we note that although the critical stress ratio μ_c and critical volume fraction ϕ_c remain insensitive to the applied pressure, the coordination numbers, both at jamming Z_c and at the flow-arrest transition Z_c, are more sensitive to the applied pressure, as seen in Figs. S3(d) and (h). At lower pressures the coordination number is consistently lower for both flowing and arrested states, which can be observed by comparing Fig. S1(c) and Fig. S2(c). Remarkably, however, the variation of ratio a_c/Z with μ is nearly equivalent at all pressures (see Fig. S1(d) and Fig. S2(d)), thus further confirming that a_c/Z is an important internal constitutive variable in modeling the flow-arrest transition of granular materials.

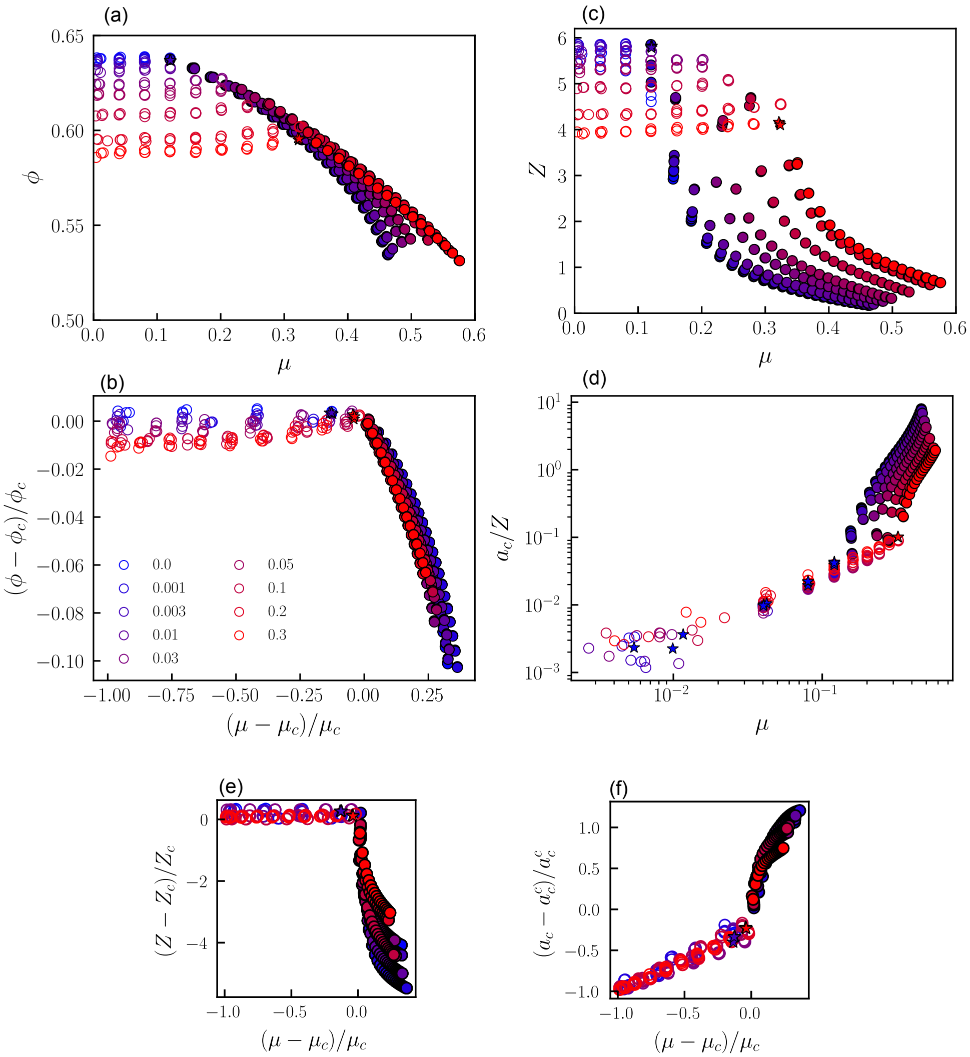

FIG. 1. (a) All simulated steady states of shear arrest (open symbols) and shear flow (closed symbols) on $\phi - \mu$ axes for all simulated interparticle frictions μ_s (see the color legend in (b)) for an applied pressure $p_a = 10^{-6}$. The asterisk denote steady states in the vicinity of the flow-arrest transition for which some simulations arrested and some steadily flowed at long times. (b) All the simulated steady states of shear arrest and shear flow in (a), with each shifted and normalized by their μ_s-dependent critical values μ_c and ϕ_c. The asterisk denote states in the vicinity of the flow-arrest transition for which some simulations arrested and some flowed steadily at long times. (b) All the simulated steady states of shear arrest and shear flow in (a) shifted and normalized by the friction-dependent critical values μ_c and ϕ_c. (d) Contact fabric anisotropy a_c normalized by Z for the states of steady flow and arrest as a function of μ. (e) All the states in (c) shifted and normalized by the friction-dependent critical values Z_c and μ_c. (f) All the states in (d) shifted and normalized by the friction-dependent critical values a_c^c and μ_c.

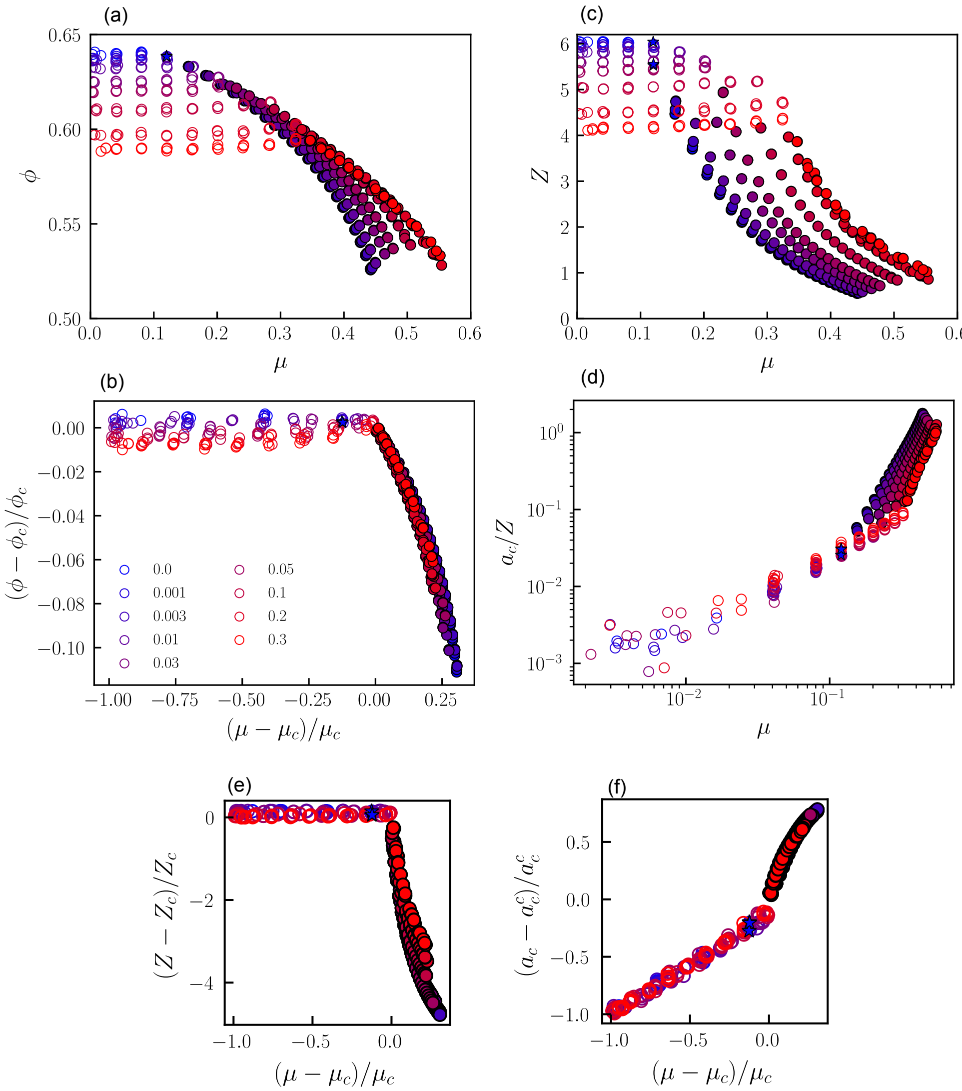

FIG. 2. (a) All simulated steady states of shear arrest (open symbols) and shear flow (closed symbols) on $\phi - \mu$ axes for all simulated interparticle frictions μ_s (see the color legend in (b)) for an applied pressure $p_a = 10^{-4}$. The asterisk denote steady states in the vicinity of the flow-arrest transition for which some simulations arrested and some steadily flowed at long times. (b) All the simulated steady states of shear arrest and shear flow in (a), with each shifted and normalized by their μ_s-dependent critical values μ_c and ϕ_c. The asterisk denote states in the vicinity of the flow-arrest transition for which some simulations arrested and some flowed steadily at long times. (b) All the simulated steady states of shear arrest and shear flow in (a) shifted and normalized by the friction-dependent critical values μ_c and ϕ_c. (d) Contact fabric anisotropy a_c normalized by Z for the states of steady flow and arrest as a function of μ. (e) All the states in (c) shifted and normalized by the friction-dependent critical values Z_c and μ_c. (f) All the states in (d) shifted and normalized by the friction-dependent critical values a_c^c and μ_c.

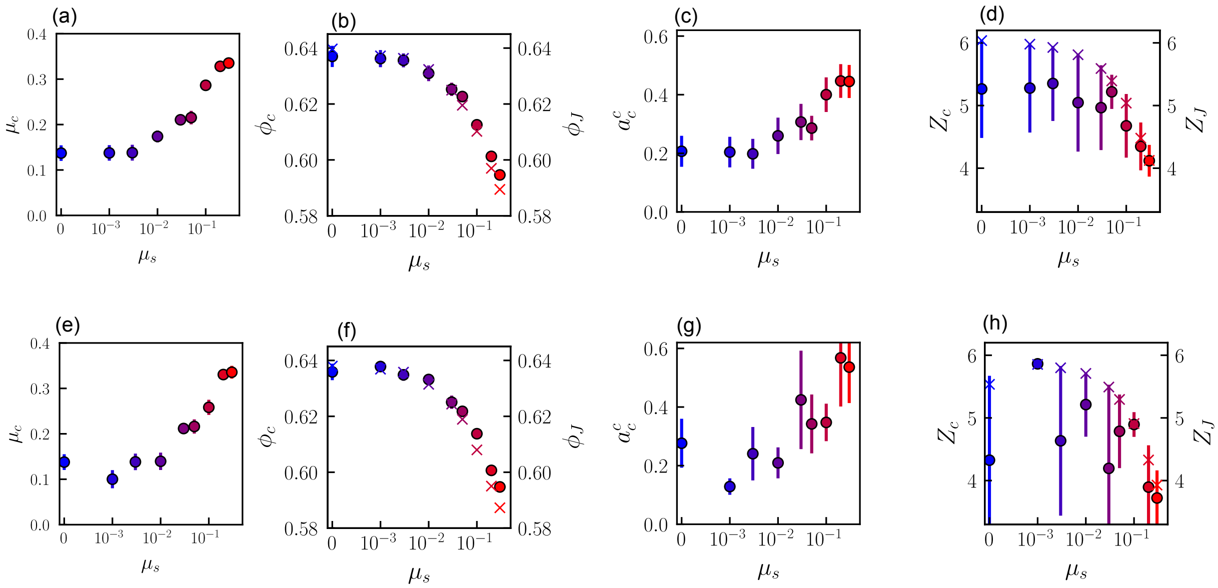

FIG. 3. Critical values (a,e) μ_c, (b,f) ϕ_c, (c,g) a_c^c and (d,h) Z_c as a function of friction μ_s. The top row corresponds to applied pressure $p_a = 10^{-4}$ and the bottom row corresponds to $p_a = 10^{-6}$. The jamming volume fraction ϕ_J and coordination number Z_J are also marked with crosses in (b,f) and (d,h) respectively. The leftmost data points in each panel correspond to the frictionless case. The vertical bars around data points represent the error in estimating the critical boundary between the steady shear flowing and shear arrested granular states from the discrete simulation data in Figs. S1 and S2.